

Diffraction from quasiperiodic unidirectional lateral superlattice observed in the geometric resonance of magnetoresistance

Akira Endo and Yasuhiro Iye

Institute for Solid State Physics, University of Tokyo, 5-1-5 Kashiwanoha, Kashiwa, Chiba 277-8581, Japan

Abstract. Magnetotransport measurement has been made on unidirectional quasiperiodic lateral superlattices in which electrostatic potential is modulated in Fibonacci sequence. We have observed (1) superposition of a series of commensurability oscillations each arising from an “average period” belonging to one of the self-similar generations and (2) geometric resonance of open orbits composed of segments of cyclotron orbits repeatedly diffracted by the quasiperiodic superlattice.

Keywords: lateral superlattice, Fibonacci, diffraction, geometric resonance

PACS: 73.23.Ad,73.21.Cd,71.23.Ft

A lateral superlattice (LSL), a genus of superlattices that is based on a high mobility two-dimensional electron gas (2DEG), represents one of the cleanest artificially modulated electron systems with the introduced length scale much shorter than the electron mean free path and offers a unique opportunity to gain precise control over the electron trajectory by using a magnetic field perpendicular to the 2DEG plane. Multitudes of interesting magnetotransport phenomena have been reported in LSL having a unidirectional periodic modulation, including the commensurability oscillation (CO) [1], the positive magnetoresistance (PMR) [2] and the quantum self-interference along closed orbits [3]. The former two can basically be understood via the properties of semiclassical electron orbits, while the closed orbits require the miniband structure formed by the Bragg reflection from the superlattice. Recently, we have reported another diffraction-related phenomenon, the geometric resonance of open orbits [4]; a small bump appears in the magnetoresistance (MR) at the magnetic field where an open orbit, a chained series of segments of cyclotron orbits diffracted repeatedly by the superlattice, have the same width as the modulation period. In the present work, we extend the study to a Fibonacci LSL (FLSL), a quasiperiodic unidirectional LSL with the potential modulated in Fibonacci sequence.

The FLSL samples were prepared from conventional GaAs/AlGaAs 2DEGs. Potential modulation was introduced by basically the same method as our previous studies [4]; by placing slabs of electron-beam resist on the surface and exploiting the strain-induced piezoelectric effect. The slabs were selectively placed on either of the “L” site (*L*-type) or “S” site (*S*-type) of the Fibonacci sequence *LSLLSLSLLSLLS...* with the width ratio $L/S = \tau = (1 + \sqrt{5})/2$ (see the inset to Fig. 1), to intro-

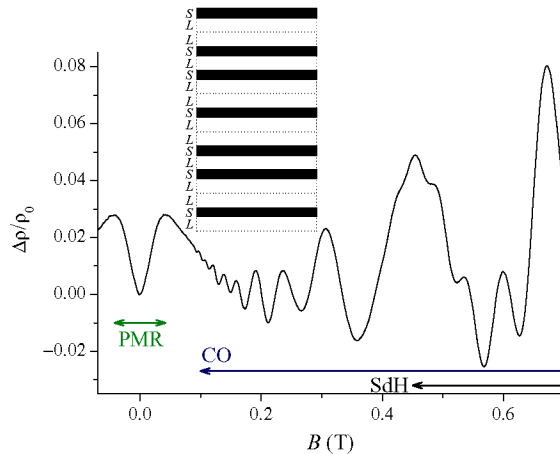


FIGURE 1. Inset: Schematic illustration of the quasiperiodic modulation pattern. Main panel: Magnetoresistance of *S*-type FLSL with $S=78$ nm and $L=127$ nm, showing PMR ($|B| < 0.042$ T), CO ($|B| > 0.1$ T), and SdH ($|B| > 0.45$ T). $T=4.2$ K.

duce quasiperiodic modulation. Several FLSL samples, both *L*-type and *S*-type, with the width of *S* ranging from 43 to 78 nm were examined.

Fig. 1 shows a typical example of the MR trace. Basically similar features as in the periodic case, PMR, CO, and the Shubnikov-de Haas (SdH) oscillation, are observed. Closer look at the CO reveals the beating of the oscillation. The beating is more clearly displayed in the inset of Fig. 2, which highlights the oscillatory part by taking the second derivative of the MR with respect to B . The Fourier transform (FT) shown in the main panel exhibits three separate peaks from CO (those marked with F1, F2, and F3) in addition to the SdH peak. The positions of the peaks appear, in the normalized coordinate

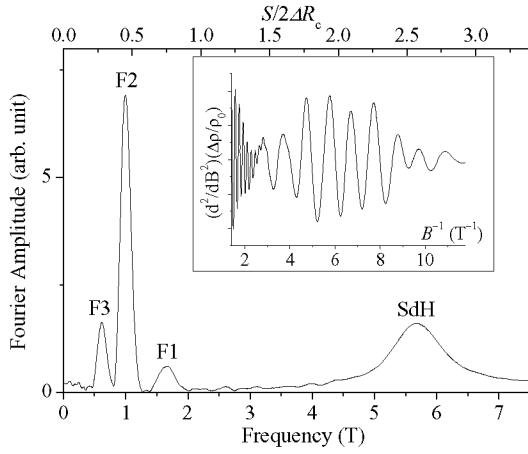


FIGURE 2. Inset: The second derivative of the magnetoresistance with respect to B plotted against B^{-1} . Main panel: The Fourier transform of the inset figure.

(top axis, obtained by multiplying $Se/2\hbar k_F$ to the bottom axis with k_F the Fermi wave number), at around 0.72, 0.45, 0.28, respectively, the ratio between adjacent peak positions being close to the golden ratio τ . In general, the FT peaks are found to appear in either of $f_j = \tau^{2-j}/\sqrt{5}$ ($j=1,2,3,\dots$), with their relative height depending on samples. The peaks for different j can be interpreted as CO corresponding to the “average period”, the average distance between adjacent troughs or ridges in the modulation potential, belonging to different self-similar generations. Note that CO is explained by drift velocity gained by a cycle of cyclotron orbit, *averaged* over the position of the guiding center [5]. A Fibonacci sequence is generated by repeating the inflation rules, $S \rightarrow L$ and $L \rightarrow LS$, starting from a single S . After a large number of steps, another inflation (or deflation) step begets a sequence similar to the previous one scaled by τ^{-1} (or τ). As can be seen in the inset of Fig. 1, the distance between adjacent S is either $S+L=\tau^2 S$ or $S+2L=\tau^3 S$. Taking into account the inflation rule and the fact that L 's occur τ times more frequently than the S 's, the “average period” is calculated to be S/f_3 . The inflation or deflation rule gives rise to average periods S/f_j , which are responsible for the observed f_j peaks in the FT spectrum.

Finally we focus on the low magnetic field region. As shown in Fig. 3, very small amplitude oscillation is superposed on the PMR, which can be clarified by taking the second derivative. As in the case of periodic modulation, we interpret that the minima in $(d^2/dB^2)(\Delta\rho/\rho_0)$ (the local maxima in MR) correspond to the positions where the width of the open orbits coincide with relevant length scales in the real space, here either $S+L$ or $S+2L$. It is well known that quasiperiodic lattice shows dense set of sharp diffraction peaks, despite the

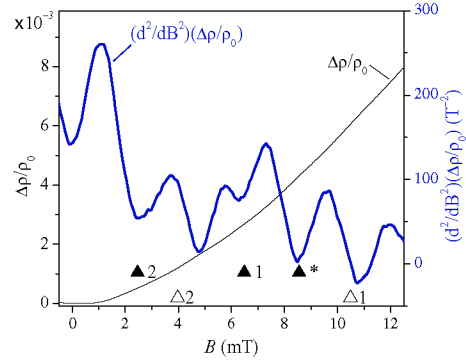


FIGURE 3. Magnetoresistance (thin line, left axis) and its second derivative (thick line, right axis) at low magnetic fields. Open and solid triangles designate the positions for the geometric resonance with $S+L$, $S+2L$, respectively, with the number (j) indicating that the diffraction f_j is responsible for the relevant open orbit. $f^*=0.83$ for the asterisk.

absence of definite periodicity (see, *e.g.*, [6]). The peak positions are given by $2\pi f/S$ with $f=(m\tau+n)/(\sqrt{5}\tau)$ for integers m, n [7]. The main contribution is given by $f=f_j$ ($j=1,2,3,\dots$), but there are other relatively large peaks, such as $f^*=0.83$ ($m=0, n=3$), which is also apparent in the numerical FT of the simulated potential profile. The diffraction generates the open orbit having the width $b=R_c[1-\sqrt{1-(\pi f/k_F S)^2}]$ with $R_c=\hbar k_F/e|B|$. Fig. 3 demonstrates that the positions are explained by the conditions $b=S+L$ or $S+2L$ reasonably well. Note that the geometric resonance is more sensitive to smaller length scale (larger f) than the CO [8].

ACKNOWLEDGMENTS

This work was supported by Grant-in-Aid for Scientific Research (C) (18540312) from Ministry of Education, Culture, Sports, Science and Technology.

REFERENCES

1. D. Weiss, K. v. Klitzing, K. Ploog, and G. Weimann, *Europhys. Lett.* **8**, 179 (1989).
2. P. H. Beton, E. S. Alves, P. C. Main, L. Eaves, M. W. Dellow, M. Henini, O. H. Hughes, S. P. Beaumont, and C. D. W. Wilkinson, *Phys. Rev. B* **42**, 9229 (1990).
3. R. A. Deutschmann, W. Wegscheider, M. Rother, M. Bichler, G. Abstreiter, C. Albrecht, and J. H. Smet, *Phys. Rev. Lett.* **86**, 1857 (2001).
4. A. Endo, and Y. Iye, *Phys. Rev. B* **71**, 081303 (2005).
5. C. W. J. Beenakker, *Phys. Rev. Lett.* **62**, 2020 (1989).
6. R. D. Diehl, J. Ledieu, N. Ferralis, A. W. Szmodis, and R. McGrath, *J. Phys.: Condens. Matter* **15**, R63 (2003).
7. V. Elser, *Acta Cryst.* **A42**, 36 (1986).
8. A. Endo, and Y. Iye, *J. Phys. Soc. Jpn.* **74**, 2797 (2005).